Supplementary Information (SI) for Physical Chemistry Chemical Physics.

Intramolecular Interaction Induced C-C Cleavages in Fructose Conversion in Polar Aprotic Solvents —— Origin of the Formation of Excess Formic Acid and Oligomers

Chenyu Ge [a], *Qianxin Sun* [a], *Ruoyu Zhang* [a], *Liangfang Zhu* [a] *and Changwei Hu*[*] [a]

[a] Key Laboratory of Green Chemistry and Technology, Ministry of Education, College of Chemistry, Sichuan University, Chengdu, Sichuan 610064, P. R. China.

AUTHOR INFORMATION

Corresponding Author

*Email: changweihu@scu.edu.cn

The PDF file includes:

Materials and Methods

Materials

All reagents were obtained from Chengdu Kelong Chemical Co., Ltd. without further purification.

Methods

In a regular reaction, a 50 mL reactor was used to study the reaction of fructose. Firstly, 50 mg D-fructose, and 10 mL MTHF were added to the reactor (purchased from Beijing Century Senlong experimental apparatus Co., Ltd). The reaction temperature was set at 120 ^{o}C and the stirring speed was 300 r min^{-1}. After the reaction, the reactor was cooled to room temperature, and the mixture was filtered. The solution was analysed qualitatively using High-Performance Liquid Chromatography (HPLC, Waters-e2695). The formulae for product-related calculations are given in Equations (1).

$$The\ mol\ yield\ of\ products = \frac{The\ mol\ of\ product}{the\ mol\ of\ fructose} \times 100\% \quad (1)$$

HPLC: The content of raw materials in the reaction solution was tested with high-performance liquid chromatography (HPLC, Waters-e2695, equipped with Bio-Rad Aminex HPX-87H Column).

Simulation Details

Molecular dynamics (MD) simulation for the minimization of each system was conducted by the steepest descent method with an emtol value of 100.0 kJ/mol^{-1}. Then NPT equilibration (where N, P, and T stand for the number of particles, pressure, and temperature) was conducted to achieve the target temperature (393 K) and real pressure for each solvent system (THF: 3.8 bar, DIO: 2.6 bar, MIBK: 3.3 bar, NMP : 1.8 bar, GVL : 1.6 bar, DMSO: 1.8 bar)[1] with md integrator (leap-frog algorithm). The time step for integration was 1 fs and the whole time for equilibration was 400 ps. The systems were all coupled from 0 K to 393 K during the first 200 ps linearly and stayed at 393 K during the rest time controlled by the simulated annealing algorithm. The Berendsen pressure coupling with a time constant of 1 ps and the V-rescale temperature coupling with a time constant of 1 ps were used in the NPT equilibration. Subsequently, the Production MD was initiated for 50 ns at 393 K and real pressure for each solvent with a time step of 1 fs with around fifty million steps in total. The Parrinello–Rahman barostat with a time constant of 4 ps and V-rescale thermostat algorithms with a time constant of 1 ps were utilized in the Production MD simulation.

Table S1. The comparison of potential transition states with H_2O assistance proton transfer steps in THF.

Transition states	Energy Barriers (kcal/mol)	
	-OH group assistance	H_2O assistance
TS3	39.07	47.37
TS5	42.51	48.66
TSh1a	44.76	58.40
TSDGE	39.13	43.53
TSf0	36.55	42.31

Table S2. The comparison of TOF (s^{-1}) for FA, FAL, HMF pathways in DIO.

Paths	FA	FAL_C3	FAL	HMF_C3	HMF_C1
TDI	Fructose	IMa2	Fructose	IMh5	Fructose
TDTS	TS1	TSDGE-1	TSh1a	TSh06	TSh1a
$\Delta G^{\ddagger}$ (kcal/mol)	43.45	43.66	44.82	43.84	44.82
ΔG_r (kcal/mol)	-27.65	-24.8	-24.8	-42.84	-42.84
TOF (s^{-1})	5.23E-12	4.04E-12	7.62E-13	1.89E-12	6.24E-13

Table S2. The comparison of TOF (s^{-1}) for FA, FAL, HMF pathways in MTHF.

Paths	FA	FAL_C3	FAL	HMF_C3	HMF_C1
TDI	Fructose	IMa2	Fructose	IMh5	IMh5
TDTS	TS1	TSDGE-1	TSh1a	TSh06	TSh06
$\Delta G^{\ddagger}$ (kcal/mol)	43.01	44.10	43.42	49.11	49.11
ΔG_r (kcal/mol)	-29.78	-54.63	-54.63	-51.06	-51.06
TOF (s^{-1})	7.50E-12	2.28E-12	5.51E-12	4.10E-15	4.11E-15

Table S3. The comparison of TOF (s^{-1}) for FA, FAL, HMF pathways in MIBK.

Paths	FA	FAL_C3	FAL	HMF_C3	HMF_C1	AA
TDI	Fructose	IMa2	Fructose	IMh5	IMh5	IMb -mibk
TDTS	TS1	TSDGE-1	TSh1a	TSh06	TSh06	TSb -mibk
$\Delta G^{\ddagger}$ (kcal/mol)	43.74	44.16	45.71	45.59	45.71	42.56
ΔG_r (kcal/mol)	-28.99	-27.79	-27.79	-46.57	-46.57	-35.96
TOF (s^{-1})	3.45E-12	2.15E-12	3.10E-13	3.18E-13	1.68E-13	1.15E-11

Table S4. The conversion of fructose in the initial reaction stage in MTHF solvent. [a]

Reaction Time	Yields [mol %]			
	HMF	FA	AA	LA
30 min	-	4.43	-	-
60 min	-	5.70	-	-

[a] Reaction conditions: 27.8 mM fructose (50 mg), MTHF solvent (10 mL), 120 ℃.

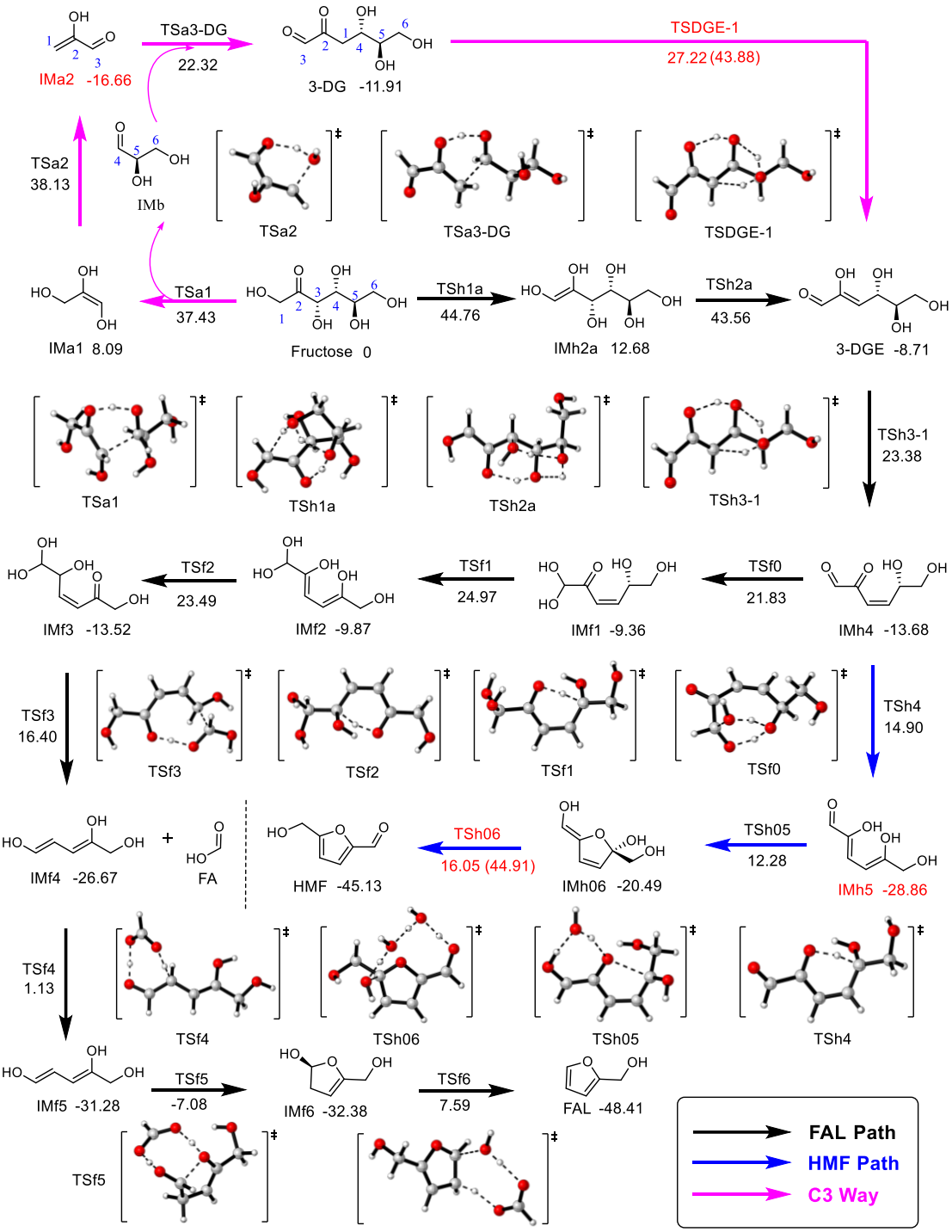

Figure S1. The detailed pathways of **HMF Path** and **FAL Path** in THF. The relative Gibbs free energy ($\Delta G/\Delta G^{\ddagger}$) data were shown in the figure with unit kcal/mol. The carbons were mainly labelled in black, and those carbons coloured in blue showed the carbon rearrangement. The RD-states for the formation of FA and HMF were coloured in red.

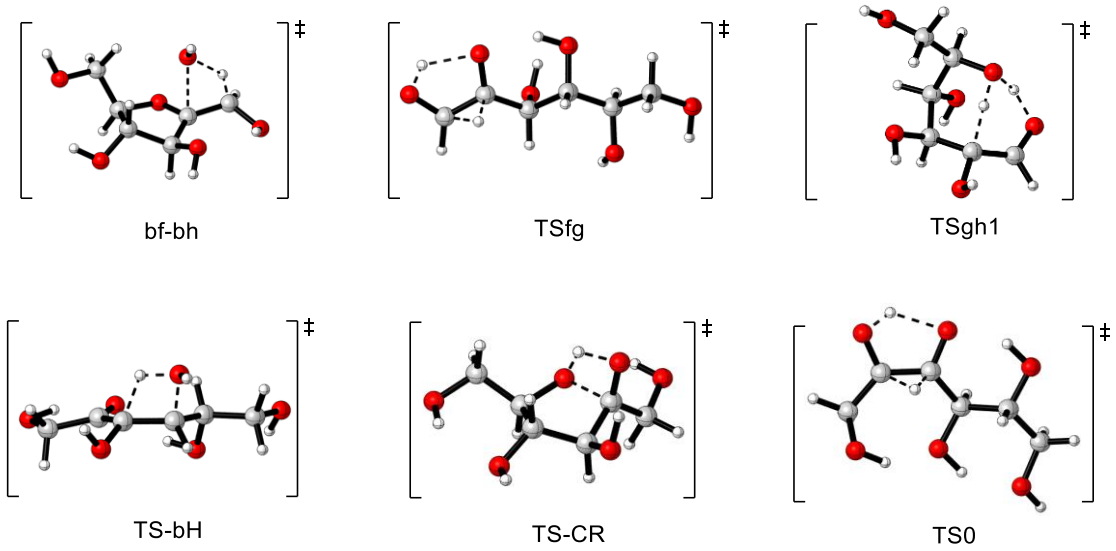

Figure S2. Transition states of other reactions of fructose in THF.

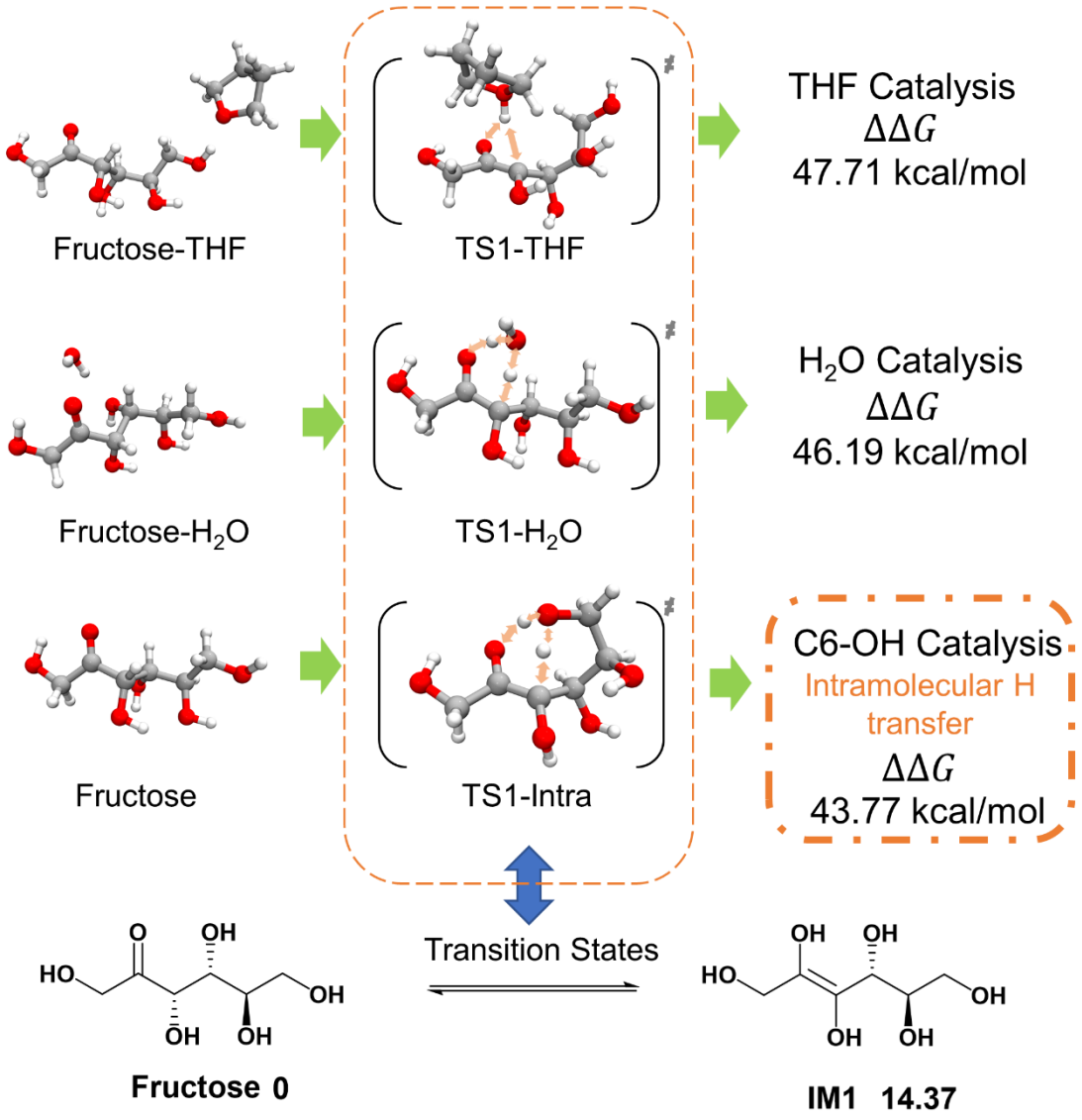

Figure S3. The comparison of THF catalysis, water catalysis and C6-OH catalysis of keto-enol tautomerization of fructose to IM1.

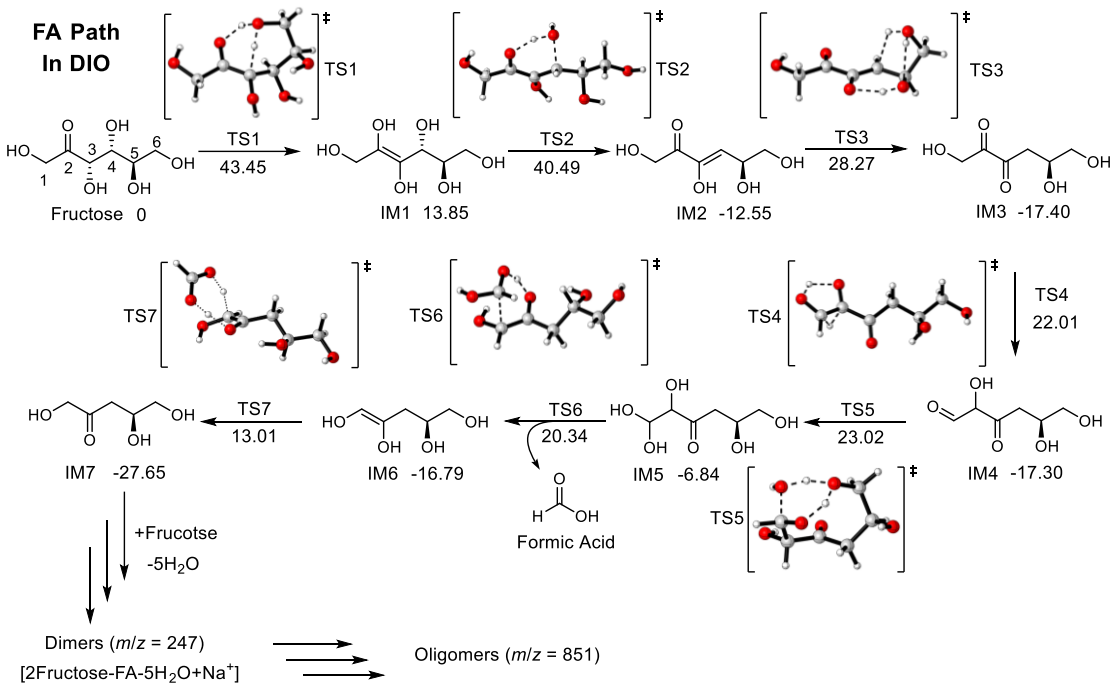

Figure S4. The reaction path and relative Gibbs free energy of FA Path in DIO solvent.

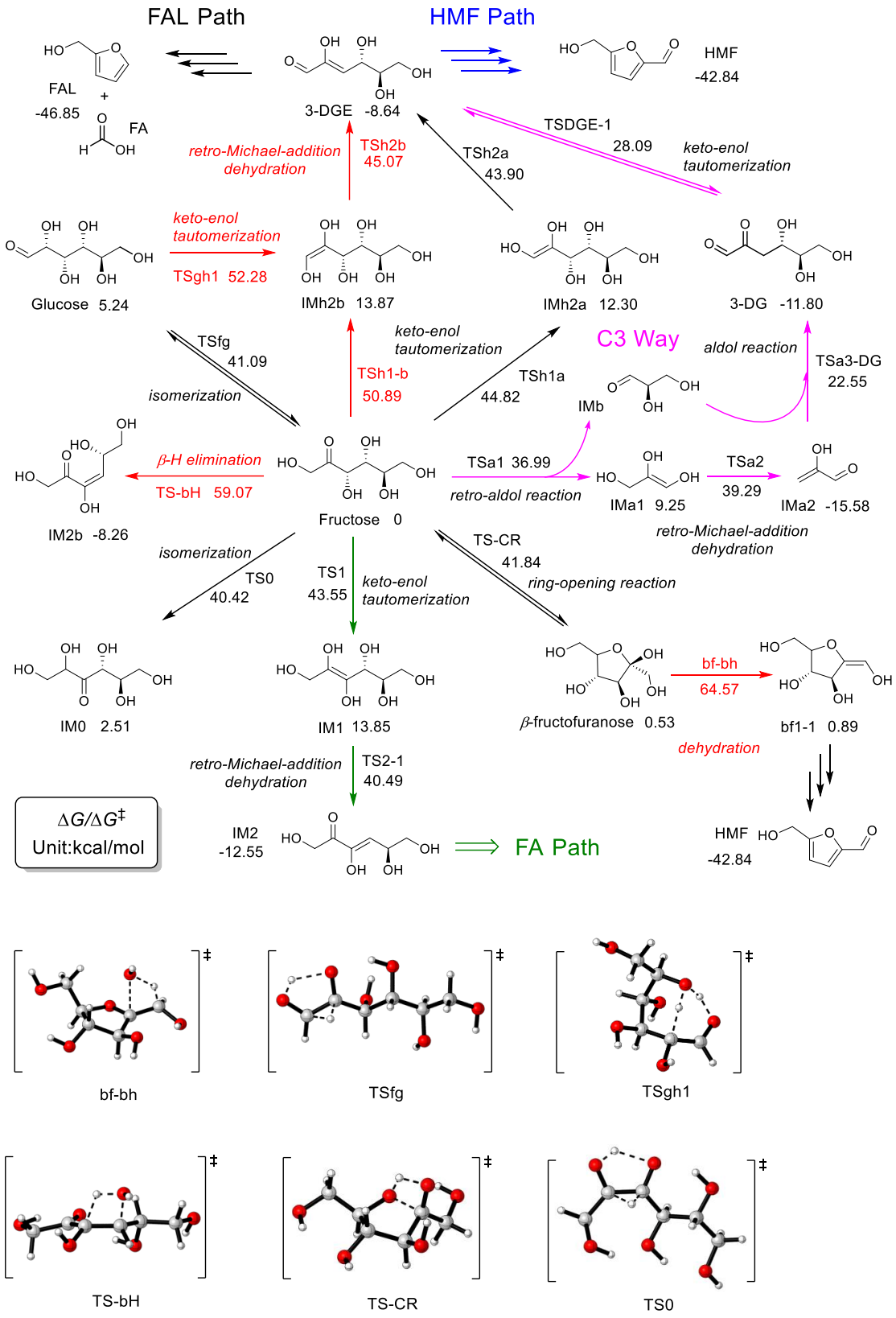

Figure S5. The possible reactions occurred to fructose in DIO solvent. The relative Gibbs free energy (**Δ*G*/Δ*G*‡**) data was shown in the figure with unit **kcal/mol**. The reaction steps with high energy barrier (above 45 kcal/mol) were coloured in red.

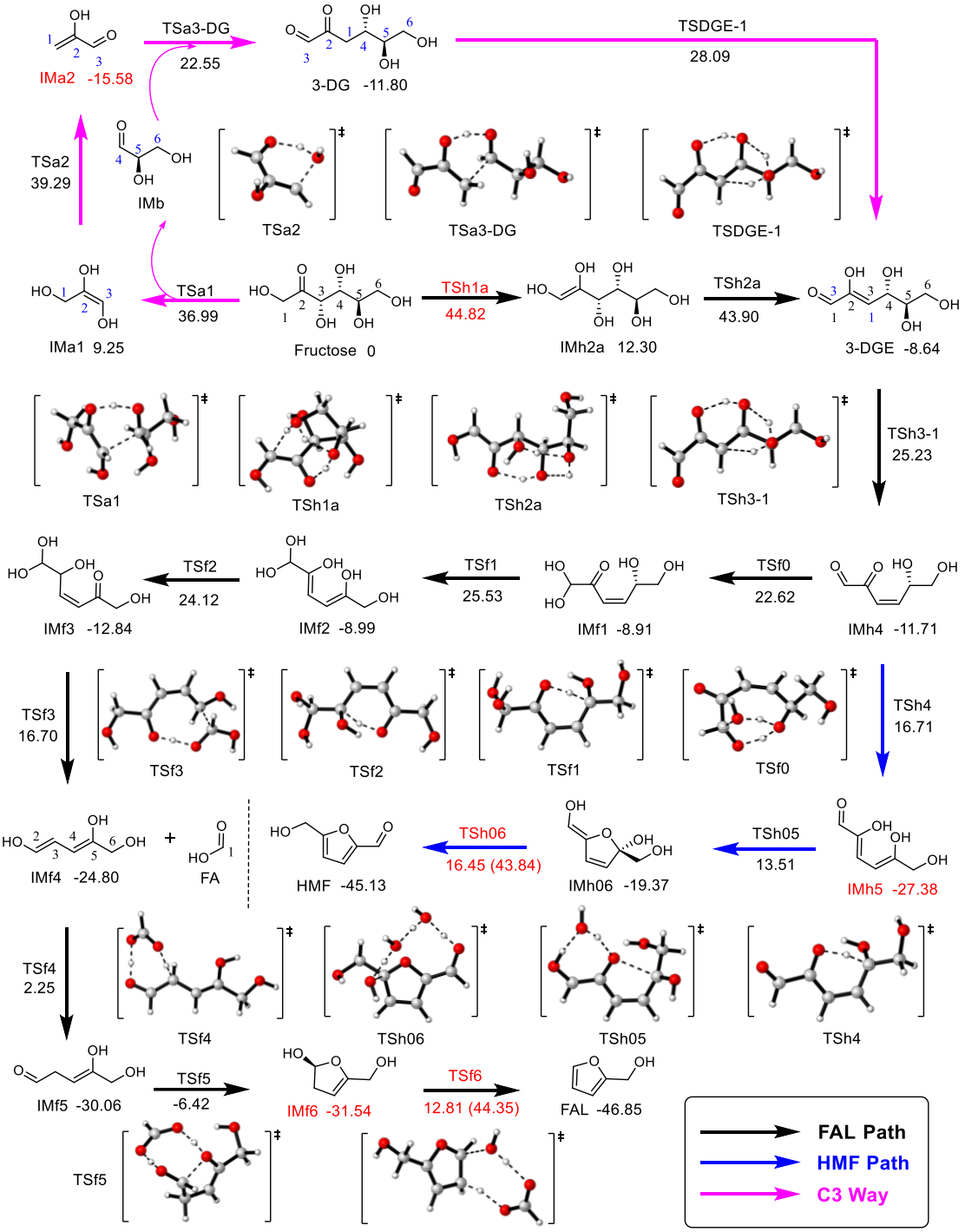

Figure S6. The detail pathways of **HMF Path** and **FAL Path** in DIO. The data of relative Gibbs free energy of structures and energy barriers ($\Delta G/\Delta G^{\ddagger}$) was shown in the figure with unit **kcal/mol**. The carbons were mainly labelled in black, and those labelled in blue showed the carbon arrangement. The RD-states for the formation of FA and HMF were coloured in red.

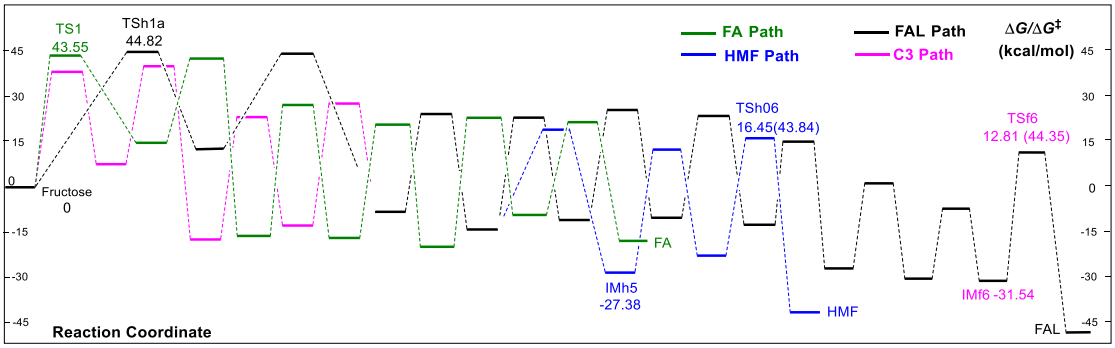

Figure S7. The potential-energy curves of reaction pathways for FA, FAL and HMF in DIO. The data of relative Gibbs free energy of structures and energy barriers (**Δ*G*/Δ*G*‡**) was shown in the figure with unit **kcal/mol**.

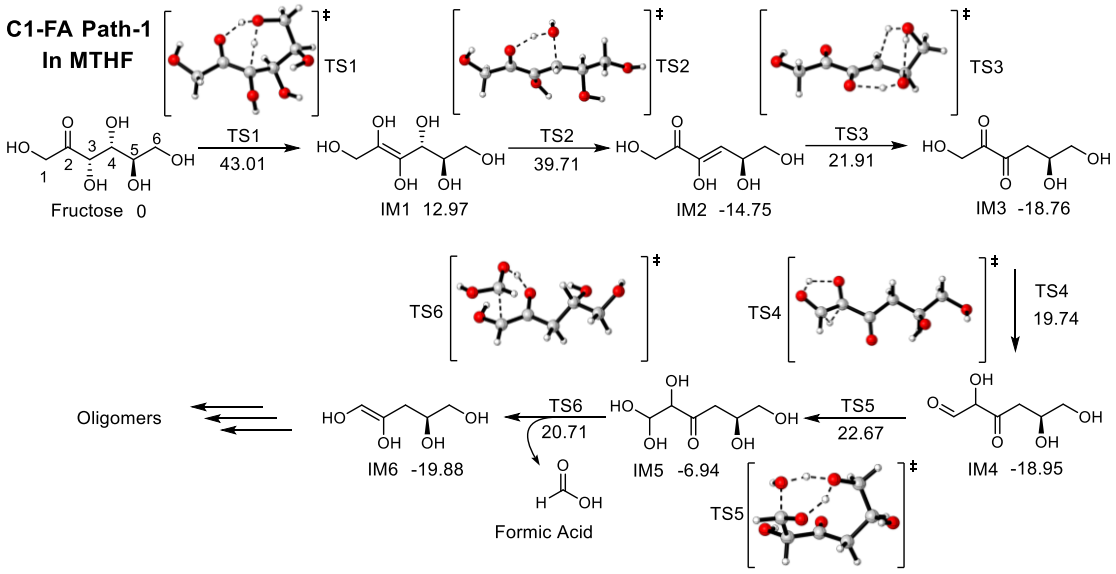

Figure S8. The reaction path of FA Path in MTHF solvent. The data of relative Gibbs free energy of structures and energy barriers ($\Delta G/\Delta G^{\ddagger}$) was shown in the figure with unit **kcal/mol**.

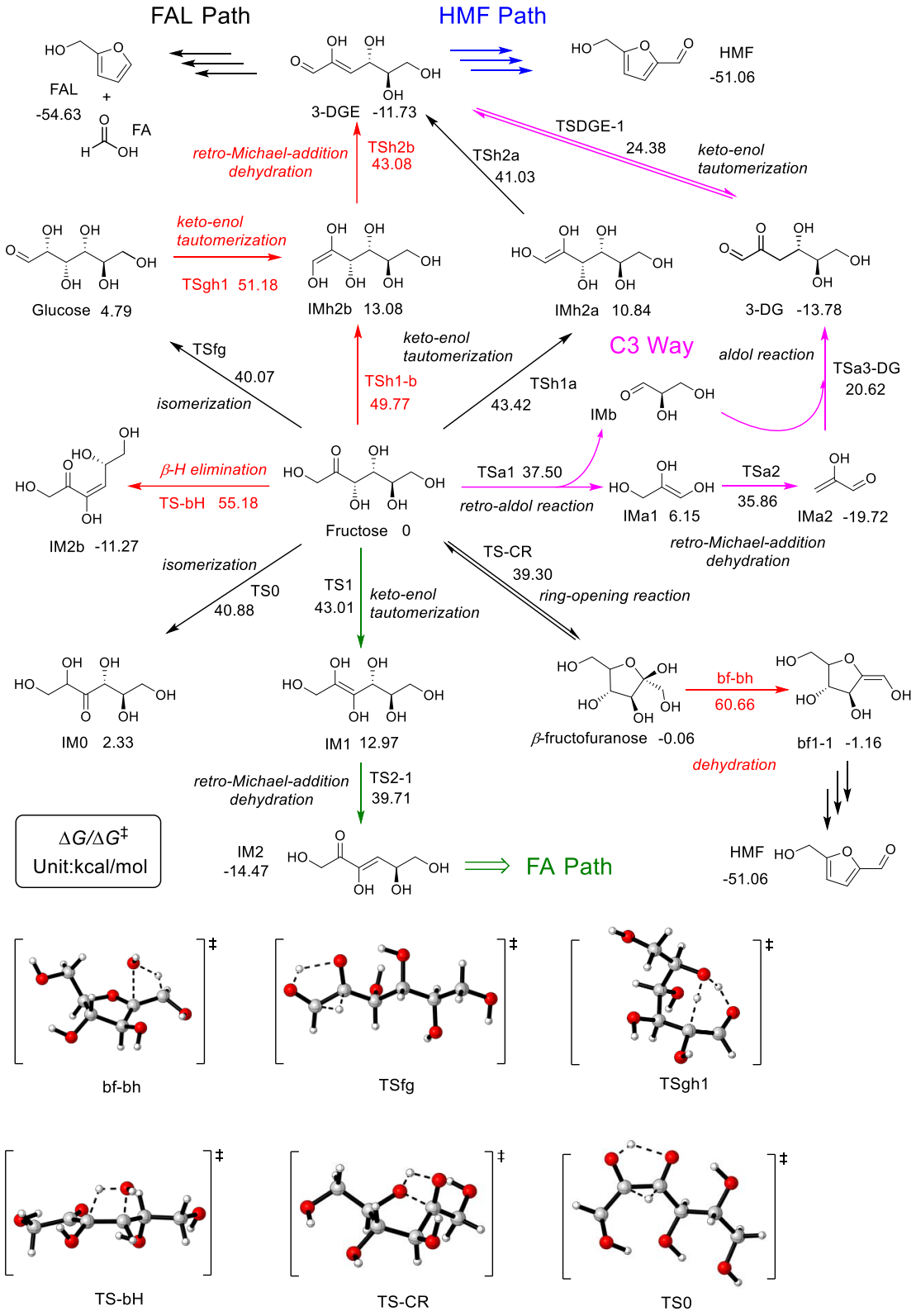

Figure S9. The possible reactions occurred to fructose in MTHF solvent. The data of relative Gibbs free energy of structures and energy barriers (**Δ*G*/Δ*G*‡**) was shown in the figure with unit **kcal/mol**. The reaction steps with high energy barrier (above 45 kcal/mol) were coloured in red.

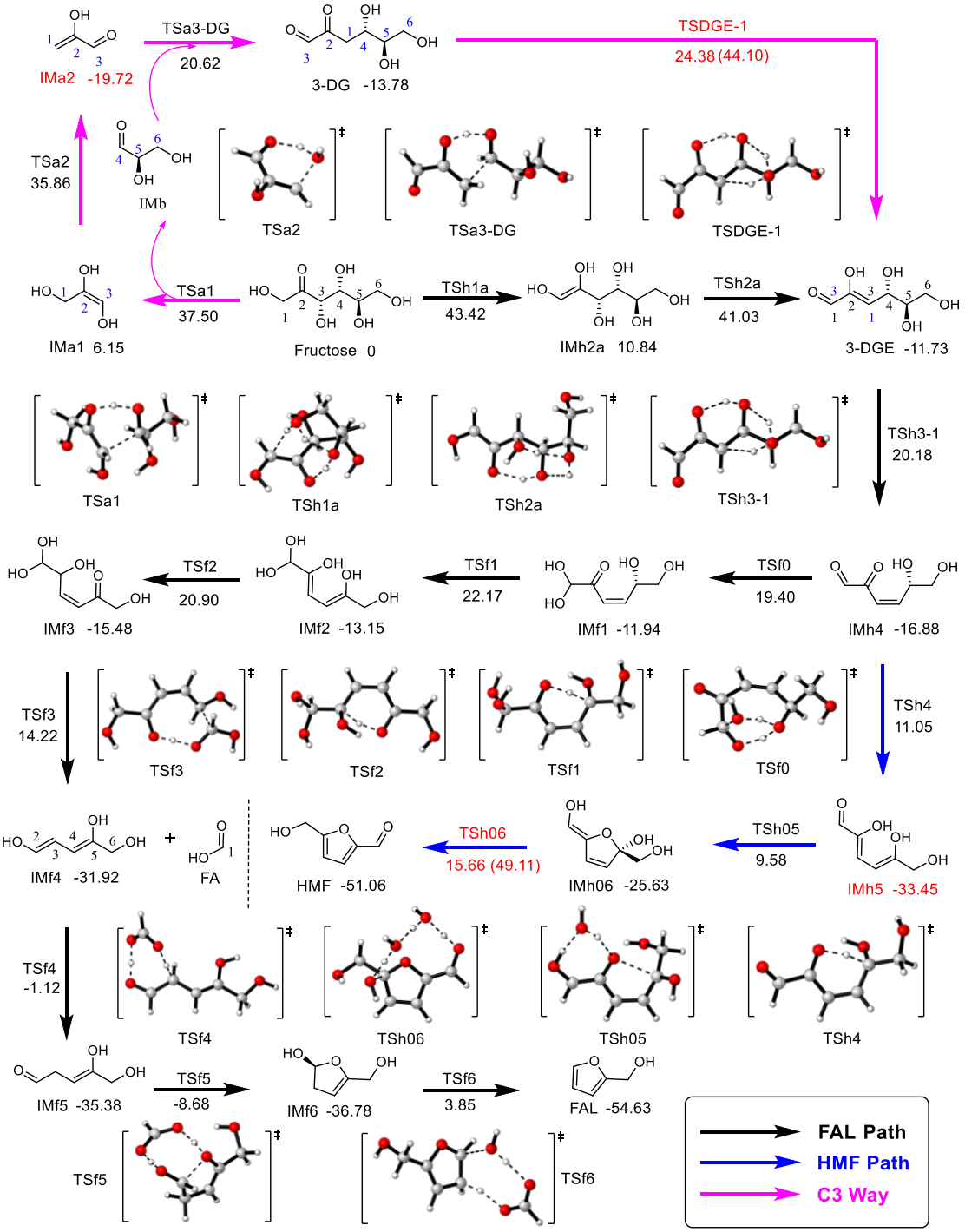

Figure S10. The detail pathways of **HMF Path** and **FAL Path** in MTHF. The data of relative Gibbs free energy of structures and energy barriers (**Δ*G*/Δ*G*‡**) was shown in the figure with unit **kcal/mol**. The carbons were mainly labelled in black, and those labelled in blue showed the carbon arrangement. The RD-states for the formation of FA and HMF were coloured in red.

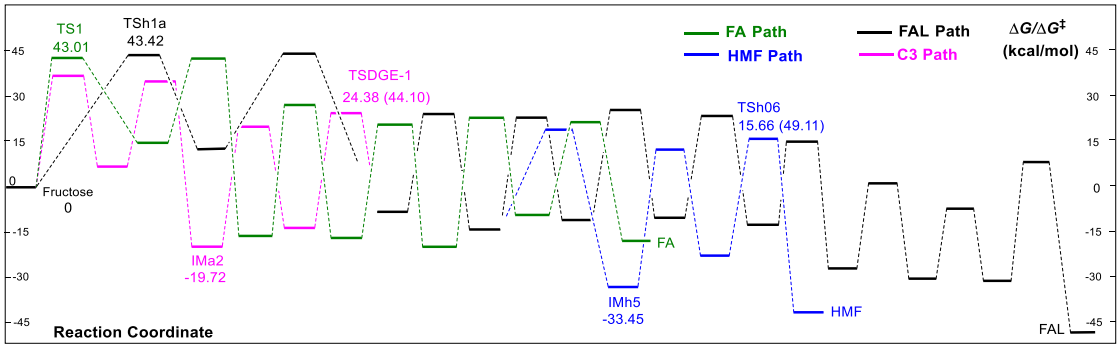

Figure S11. The potential-energy curves of reaction pathways for FA, FAL and HMF in MTHF. The data of relative Gibbs free energy of structures and energy barriers (**Δ*G*/Δ*G*‡**) was shown in the figure with unit **kcal/mol**.

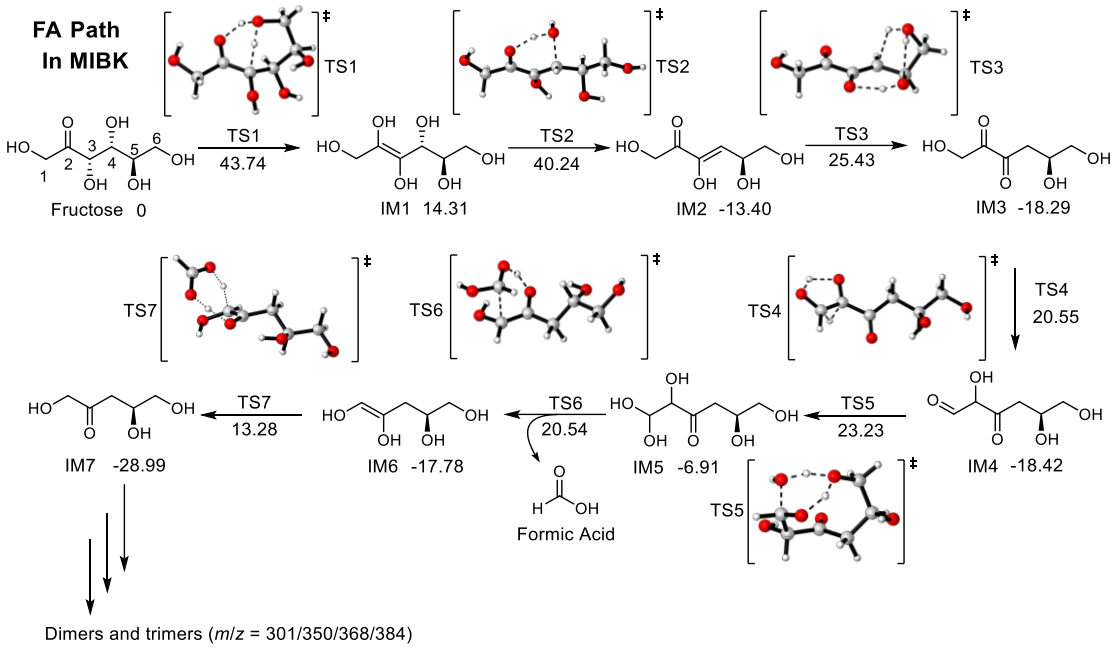

Figure S12. The reaction path of FA Path in MIBK solvent. The data of relative Gibbs free energy of structures and energy barriers ($\Delta G/\Delta G^{\ddagger}$) was shown in the figure with unit **kcal/mol**.

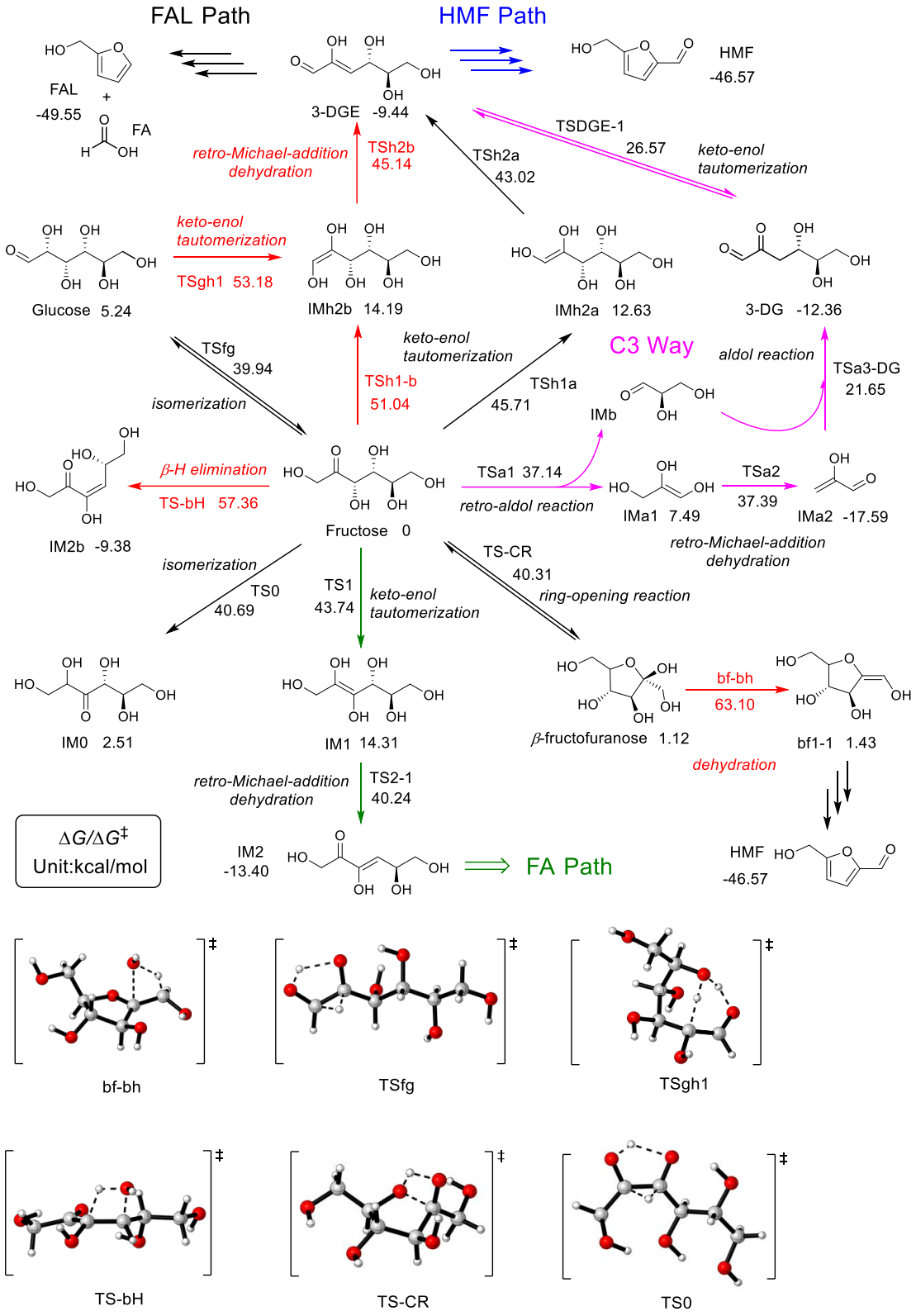

Figure S13. The possible reactions occurred to fructose in MIBK solvent. The data of relative Gibbs free energy of structures and energy barriers (**Δ*G*/Δ*G*‡**) was shown in the figure with unit **kcal/mol**. The reaction steps with high energy barrier (above 45 kcal/mol) were coloured in red.

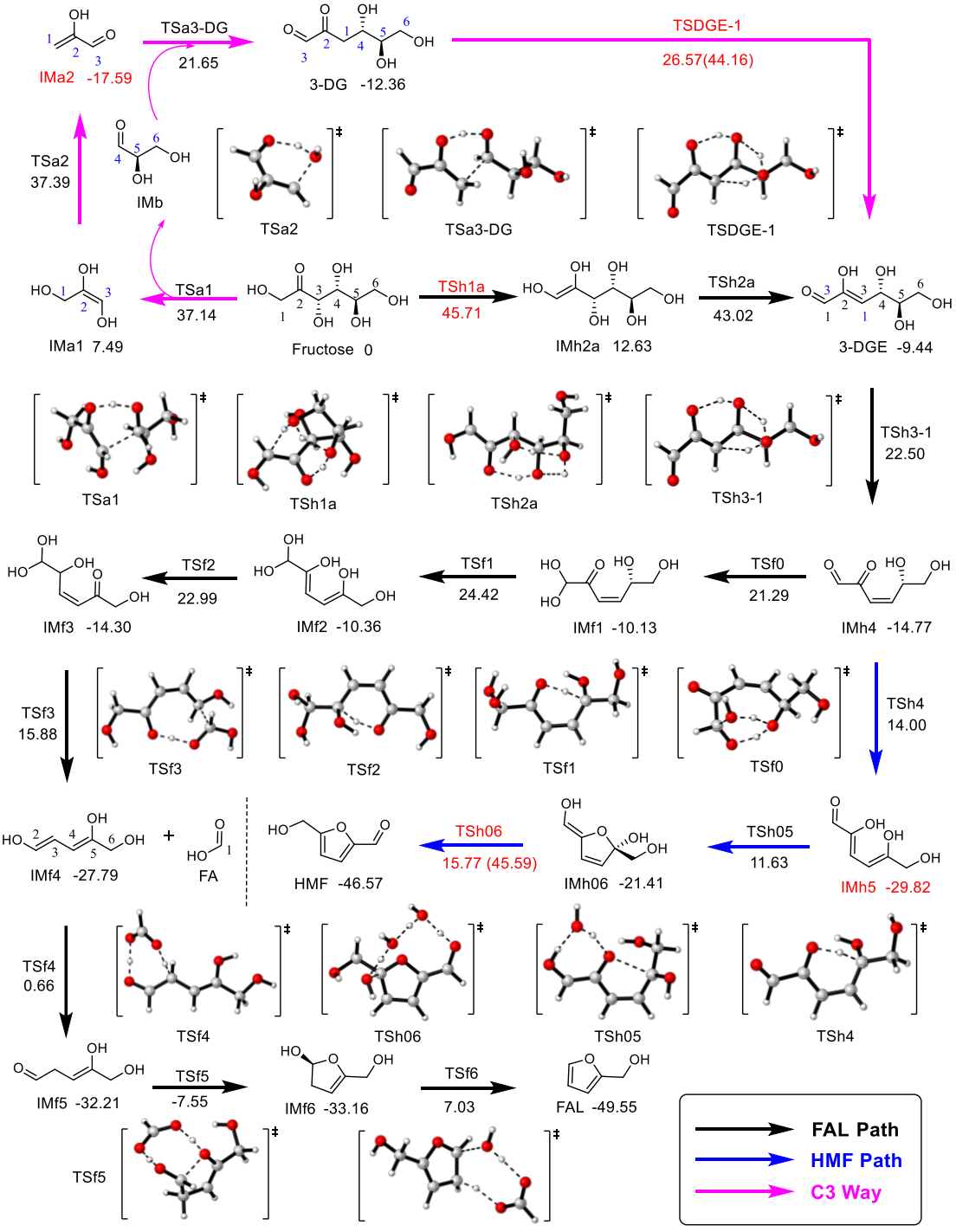

Figure S14. The detail pathways of **HMF Path** and **FAL Path** in MIBK. The data of relative Gibbs free energy of structures and energy barriers (**Δ*G*/Δ*G*‡**) was shown in the figure with unit **kcal/mol**. The carbons were mainly labelled in black, and those labelled in blue showed the carbon arrangement. The RD-states for the formation of FA and HMF were coloured in red.

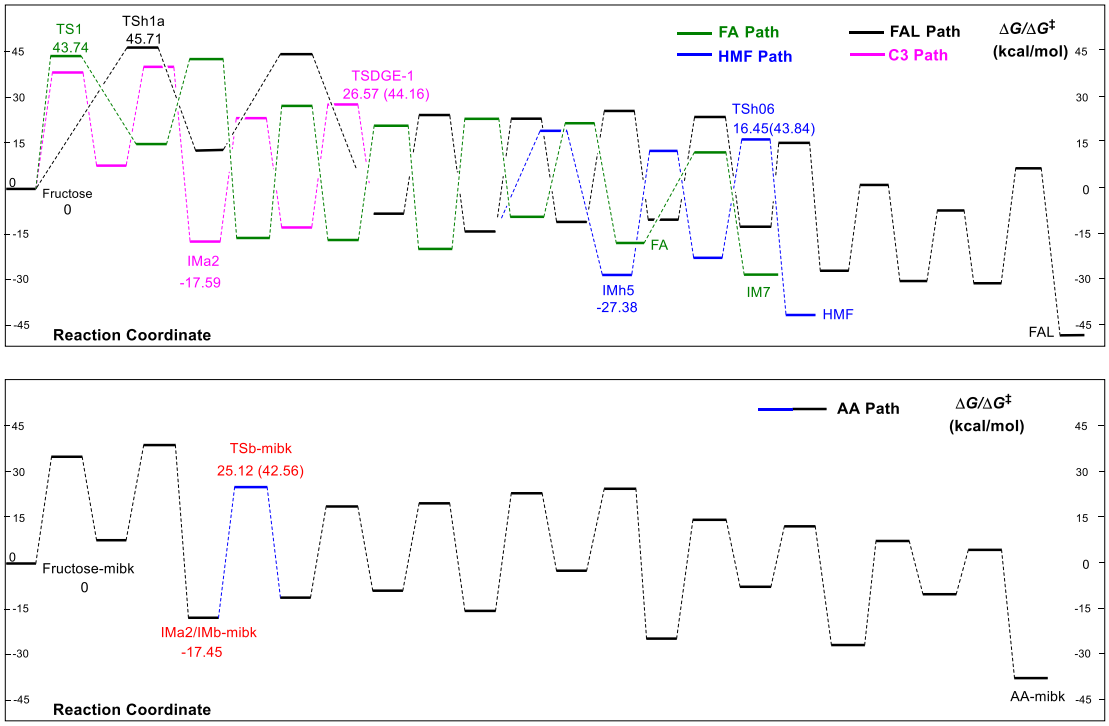

Figure S15. The potential-energy curves of reaction pathways for FA, FAL, HMF and AA in MIBK. The data of relative Gibbs free energy of structures and energy barriers (**Δ*G*/Δ*G*‡**) was shown in the figure with unit **kcal/mol**.

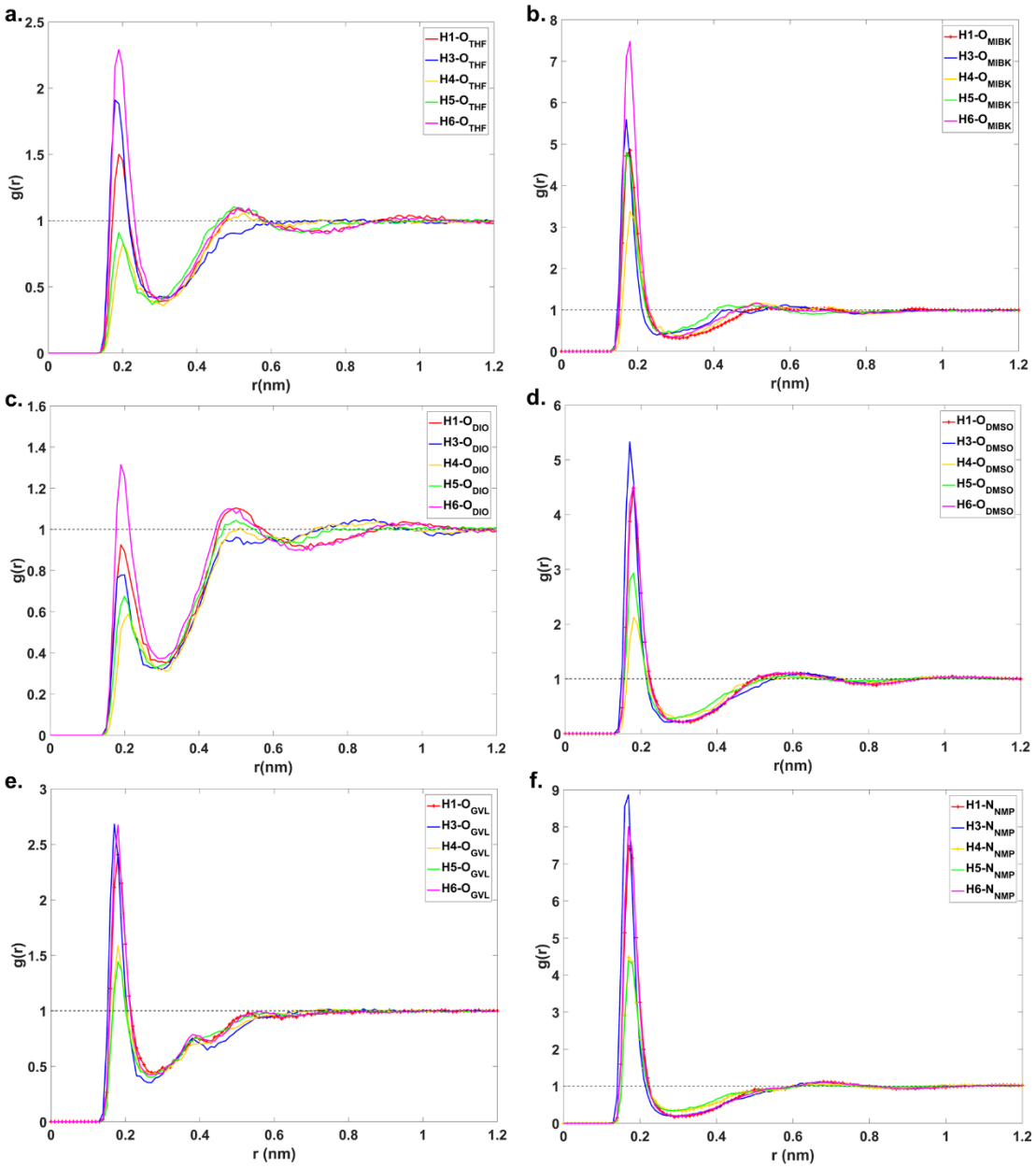

Figure S16. The RDF curves of O atom (N atom for NMP) on solvents from hydroxyl H atoms on fructose in different solvent. The hydroxyl H on Cn was labelled as Hn. a. THF. b. MIBK. c. DIO. d. DMSO. e. GVL. f. NMP.

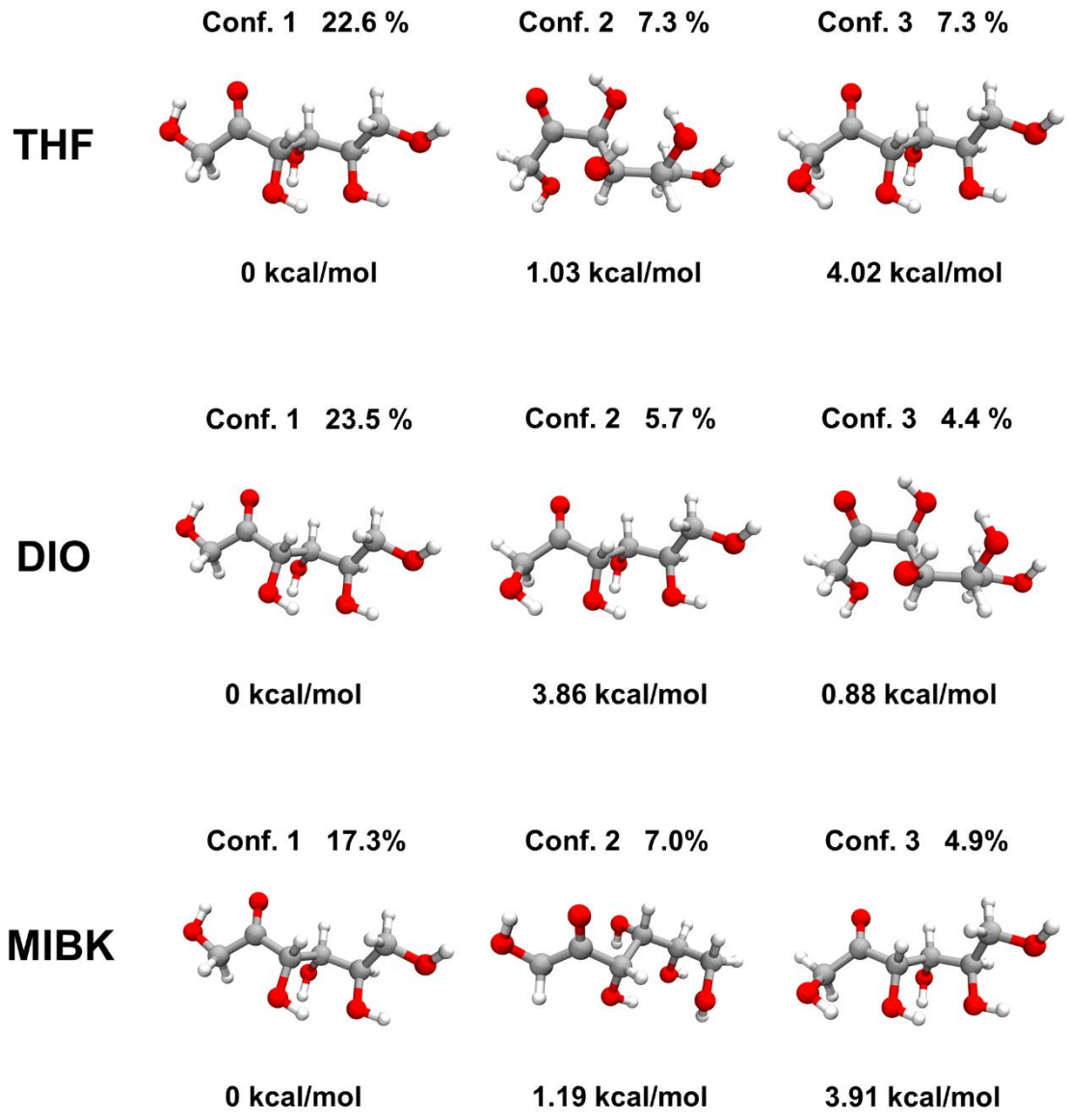

Figure S17. The first three main conformations of chain fructose in THF, DIO and MIBK solvent.

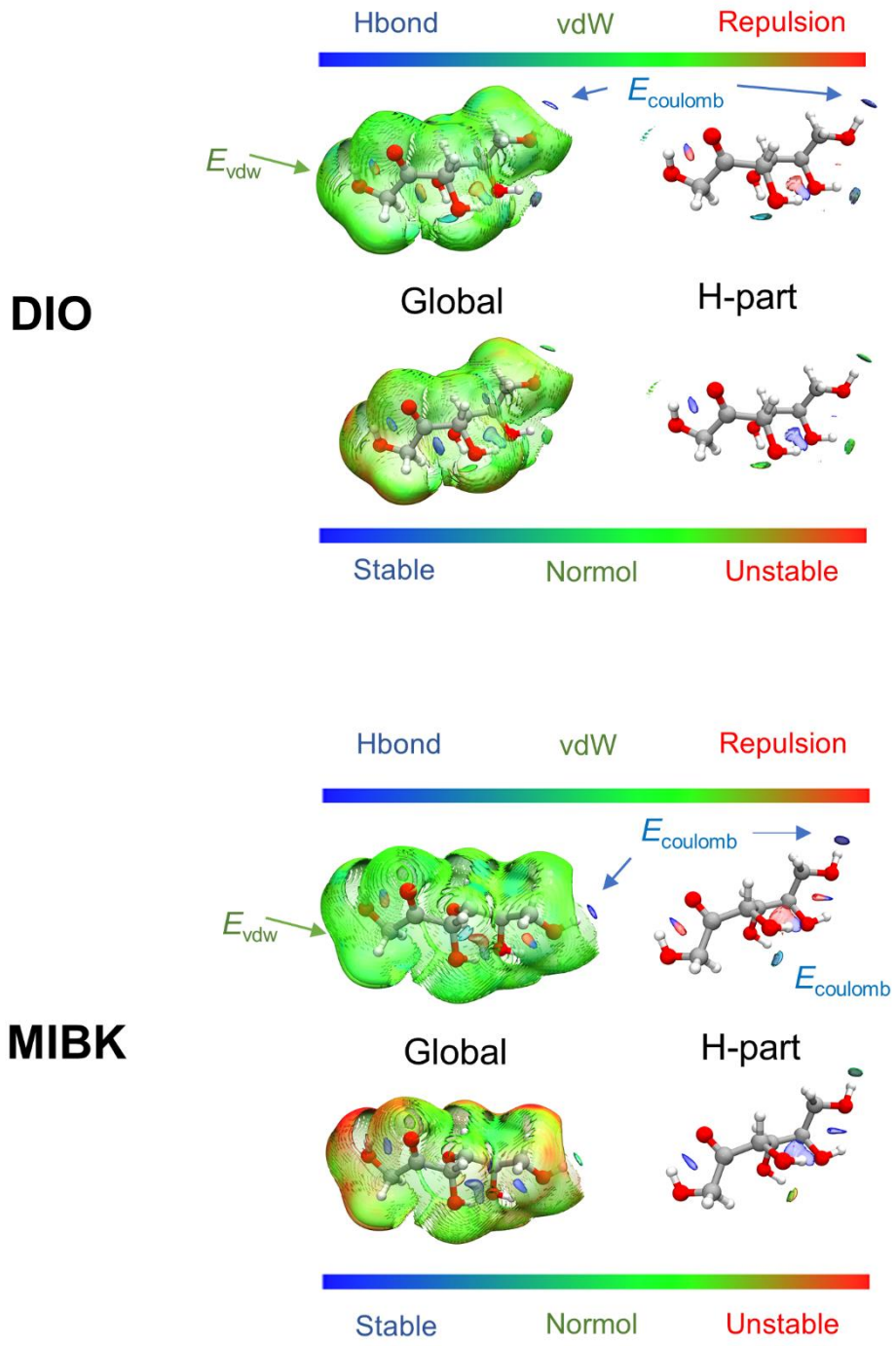

Figure S18. aNCI (above) and TFI (below) analysis for main conformation of acyclic keto D-fructose in DIO and MIBK solvent. Global showed the whole interactions around fructose, and to make the interactions of H-bonds more clearly, H-part showed the interactions around hydroxyl H atoms only.

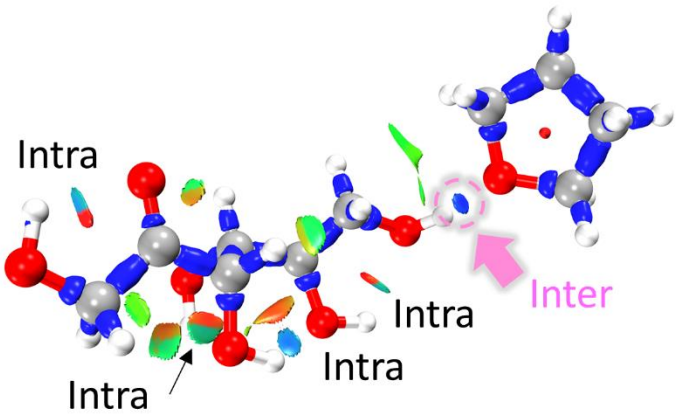

Energy Decomposition Analysis for Intermolecular H-bond

Frag.	Electrostatic	vdW		Total
		Repulsion	Dispersion	
Frucose-THF	-40.27	18.26	-19.14	-41.16

Figure S19. Visualization of weak interactions and chemical bond interactions of main conformation keto-D-fructose in THF. Energy decomposition analysis for intermolecular H-bond based GAFF force filed (unit: kJ/mol).

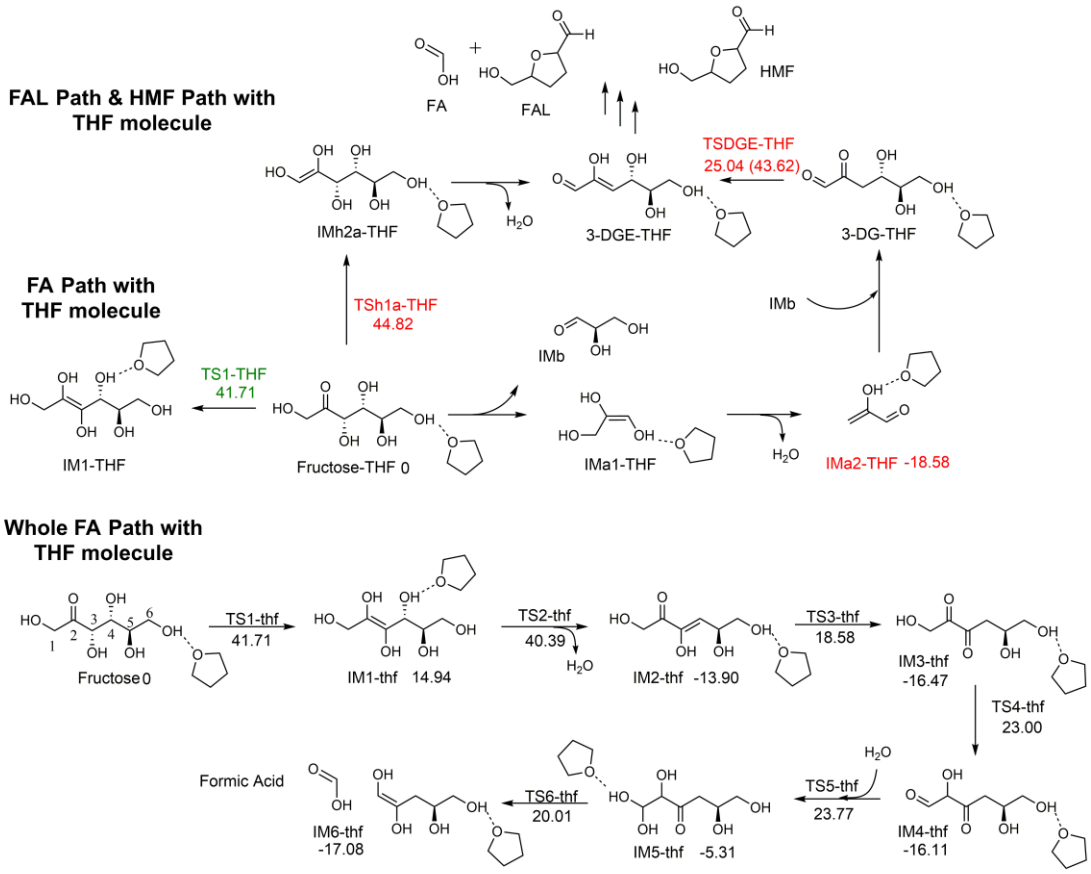

Figure S20. Main reaction pathways with THF explicit solvent molecule in THF. Relative Gibbs free energy unit: kcal/mol.

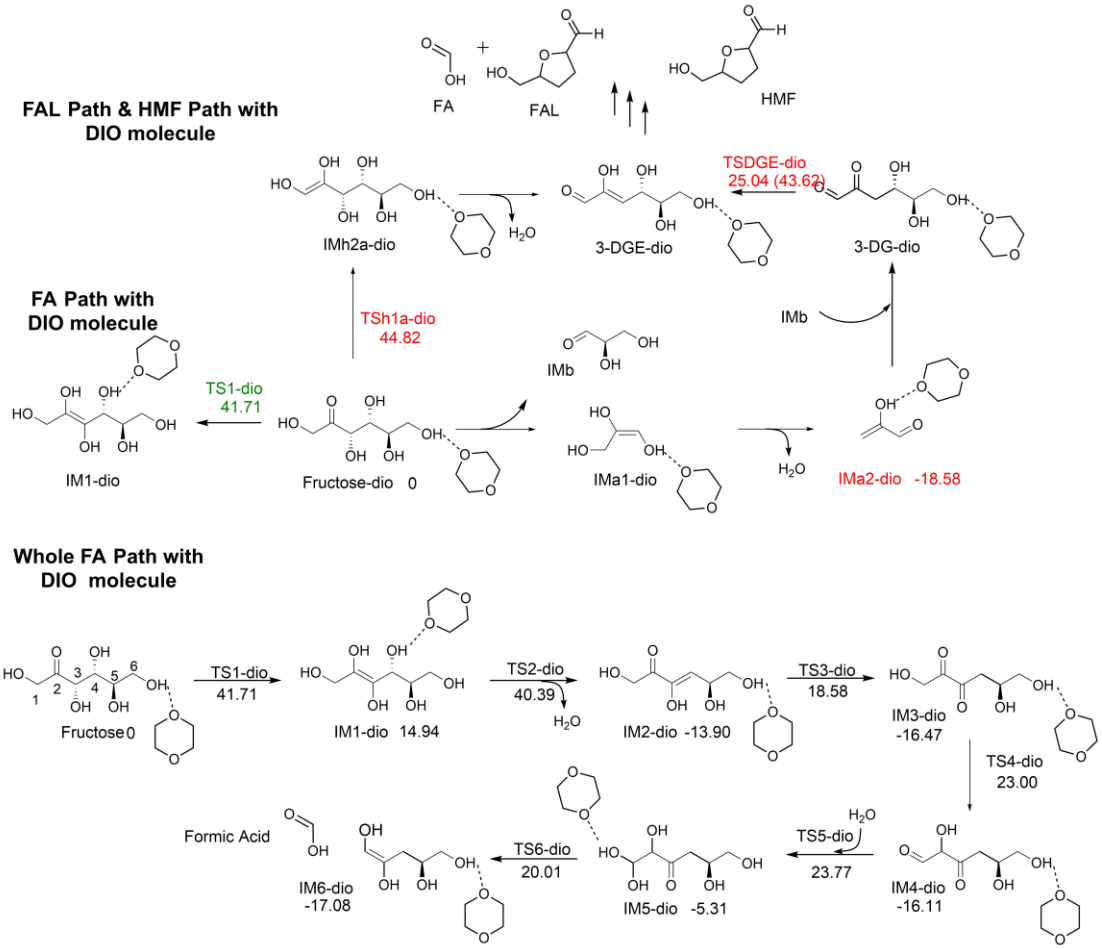

Figure S21. Main reaction pathways with DIO explicit solvent molecule in DIO. Relative Gibbs free energy unit: kcal/mol.

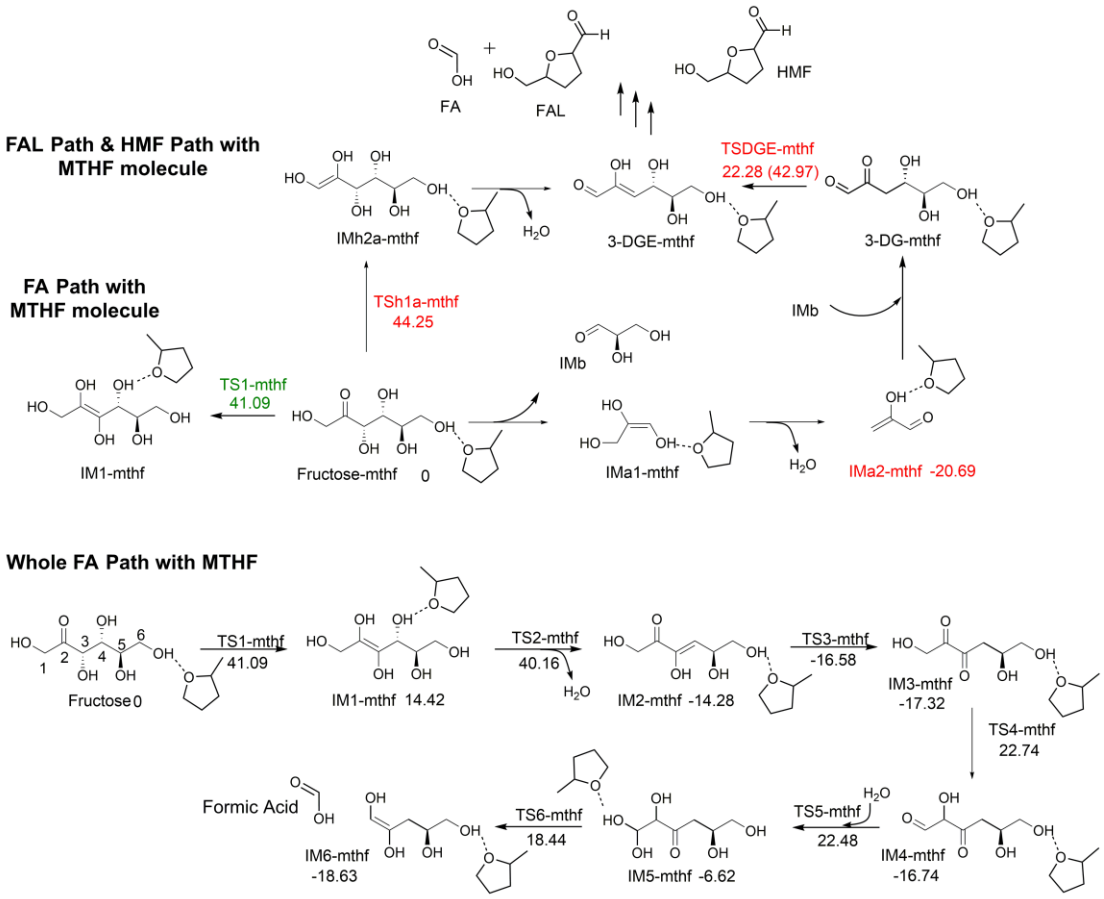

Figure S22. Main reaction pathways with MTHF explicit solvent molecule in MTHF. Relative Gibbs free energy unit: kcal/mol.

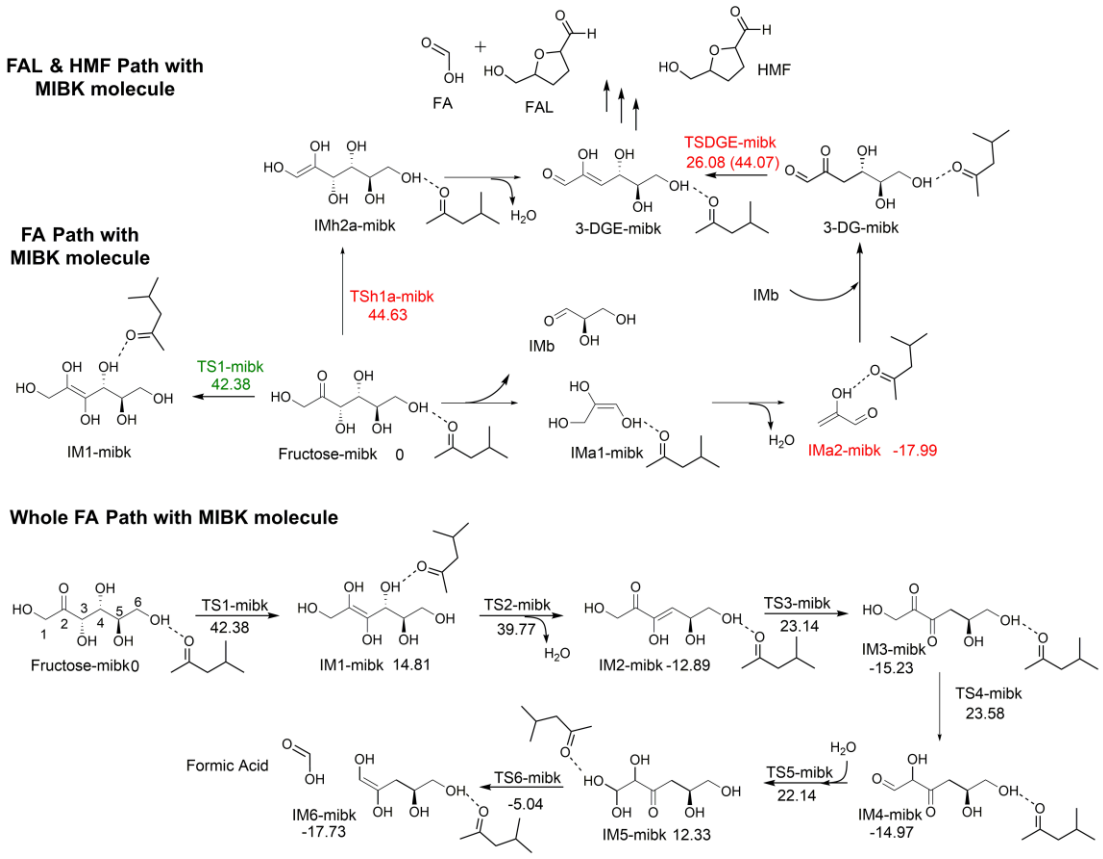

Figure S23. Main reaction pathways with MIBK explicit solvent molecule in MIBK. Relative Gibbs free energy unit: kcal/mol.

Reference

1. X. Fu, Y. X. Hu, Y. R. Zhang, Y. C. Zhang, D. Y. Tang, L. F. Zhu and C. W. Hu, *Chemsuschem*, 2020, **13**, 501-512.